Investigation of the Effect of Steel Plate Size and Elevated Temperature on Critical Load in Stability Tests

O.A. Pashkov[1]

[1]Moscow Aviation Institute (National Research University), Volokolamskoe shosse, 4, 125993, Moscow, Russia
[1]oapashkov@mail.ru

Abstract : This paper presents the results of a study of the effect of epoxy-polyester-based powder coatings on the critical strength of plate samples made of rolled sheet steel. The results obtained show that the model using flat elements gives a more accurate result than the model using three-dimensional elements. The best agreement with the experiment was shown by the results obtained in Ansys using the Eigenvalue bucling function, less than 1%. The worst agreement with the experiment was shown by the results obtained in Ansys using Solid elements, about 70%.

1. Introduction

Preliminary experiments have shown that when studying the mechanical properties of samples of metal plates and metal plates with applied polymer coatings at elevated temperatures in stability tests, only the coated samples are affected [1-18]. Creation of polymer coatings on the surface of planar and spherical substrates becomes increasingly important and has attracted a great deal of attention of a gange of researchers [19-41]. Therefore, the purpose of this work was to perform a numerical and analytical calculation of the stability of samples of metal plates with polymer coatings. An analytical calculation was carried out for samples at room temperature using the Euler formula [42-44]. Numerical calculation was carried out in Ansys software for batches of samples at room and elevated temperatures [45-48].

2. Experimental studies of coating samples

Samples were considered from rolled sheet steel with a constant thickness of 0,7 mm and, depending on the batch, of various lengths and widths without coating and with it. Powder coating on epoxy-polyester base EUROPOLVERI (RAL 9010, Italy) with a thickness of about 250 microns with a spread of values of ± 30 microns was applied electrostatically. Before applying coatings, the steel surface was degreased and phosphated. Coating was carried out in a Gema paint booth (Switzerland). Drying was carried out at a temperature of 120 °C for no more than 5 minutes. Polymerization of the sprayed layer was carried out in a heat chamber at a temperature of 150 °C for 30 min. Samples were cooled in air for several hours.

The length of the working zone for specimens with a length of 240 mm was 131,85 mm, and for specimens with a length of 120 mm – 86,15 mm. For calculations, the length of the working zone was taken as 132 mm and 86 mm, respectively. The samples were tested at a constant speed of 0,5 mm/min. Mechanical grips were used for all samples. When tested with an elevated temperature, the sample was held for 10 minutes.

It was assumed that in the process of heating, the coated sample is weakened in the grips due to softening of the coating, and additional effort is required to fix the sample. For this confirmation, the effect of additional pulling up of mechanical grips was investigated in the stability test at elevated temperatures. The difference between the tests with and without pulling up consisted only in the fact that during the pull-up test the sample was additionally pulled up 5 minutes after reaching 80°C After additional tightening, the sample was kept for another 5 minutes at the same temperature. Samples without pulling up were kept at 80°C for 10 minutes. For this study, 6 samples were considered in each batch:

Uncoated batch with sample size 240*24*0,9
Coated batch and sample size 240*24*1
Uncoated batch with sample size 120*24*0,9
Coated batch and sample size 120*24*1

This study showed the need for additional pull-up of coated samples. Therefore, all other coated samples were tightened after 5 minutes at a temperature 80 °C.

Twelve batches were considered to study the effect of the coating on the critical force in the elevated temperature test. Each batch consisted of 5 samples, each sample was kept at a temperature of 80°C for 10 minutes. The coated lots were additionally pulled up. The following batches have been tested:

Uncoated batch with sample size 240*24*0,7
Coated batch and sample size 240*24*1,2
Uncoated batch with sample size 120*24*0,7
Coated batch and sample size 120*24*1,2
Uncoated batch with sample size 120*12*0,7
Coated batch and sample size 120*12*1,2

Mechanical tests were carried out on an Instron 5969 setup (UK) with Bluehill 3 software. For numerical simulation of buckling tests, standard methods of finite element analysis in the Ansys system were used.

3.　Methods and results of numerical modeling

In the calculations, the following values of the physical and mechanical properties of the samples were used:
Sheet steel: Elastic modulus E = 200 GPa, Poisson's ratio μ= 0,3, Coefficient of thermal expansion α=12.5*10^{6}C^{-1}, EUROPOLVERI coating: Elastic modulus E = 3 GPa, Poisson's ratio μ= 0,03, Coefficient of thermal expansion α=55*10^{-6}C^{-1}.

In the numerical calculations, the possible curvature of the sample was taken into account by setting the initial curvature by the radius. When calculating for an elevated temperature, polymerization at a temperature of 150°C was taken into account, taking the temperature change relative to the neutral state equal to -70 ºC.

Ansys built a curved surface with a curvature of a radius of 1 * 107mm. Two variants of modeling experimental samples were considered: by two-dimensional modeling: the surface was broken by two-dimensional QUAD elements; and 3D modeling: solid was broken by 3D Hex elements. To simulate anchoring similar to the experiment, the boundary conditions were set: The lower face was set to the termination conditions (prohibition of displacements and turns in all directions). The conditions for prohibiting displacements in the direction of the width Ox and thickness Oz of the sample, as well as rotation around the direction of the width of the sample Rx, were set on the upper face. The load was applied to the upper face along the Oy axis in the form of a force. The coverage was modeled by the layered section function.

The value of the critical force is determined from the formula of the theory of bar stability for the case of vertical load action and rigid pinching of the ends of the bar:

$$P_{кр} = \frac{4\pi^2 EJ}{l^2} \text{ ,}$$

where $l = 86$ мм – rod length, E – Young's modulus, J – moment of inertia of the cross-section of the bar.

When modeling plates without coatings, we take $E = E_{cm}$ – Young's modulus of steel, $J = J_{cm} = bh^3/12$ – moment of inertia of samples with thickness h and width b. When modeling plates with coatings, the stiffness of the corresponding bar in bending should be calculated taking into account the additional contribution from the coating layers: $EJ = 2E_n J_n + E_{cm} J_{cm}$, where E_n - is the modulus of elasticity of the coating, J_n – is the moment of inertia of the coating layers displaced relative to the neutral line of the bar. However, the use of such a refined estimate leads to an insignificant change in the calculated critical load (within 2%), which cannot explain the obtained experimental data. Therefore, the graphs show the only value of the critical load, calculated without taking into account the effect of coatings.

The dependence of the curvature of the sample on the critical load is shown in the figure 1.
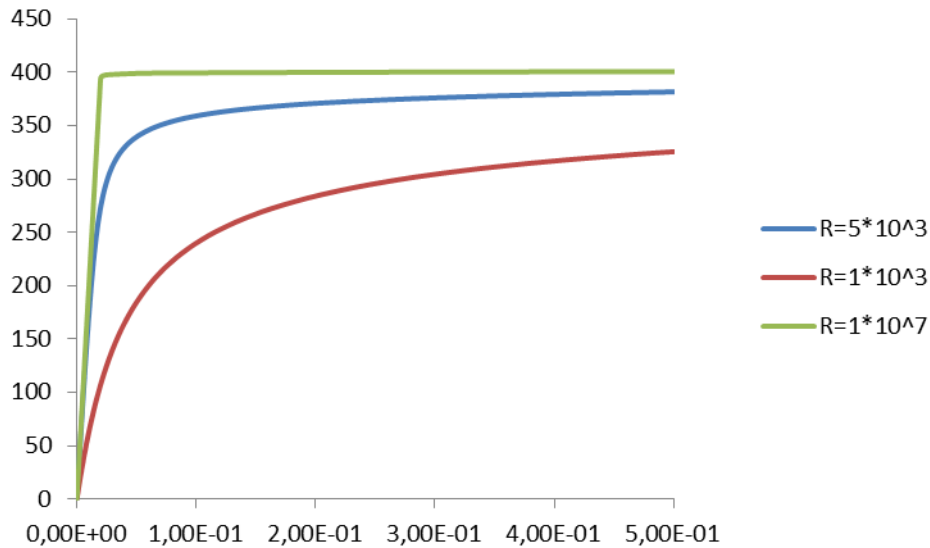
Fig. 1. Dependence of the critical load on the given curvature of the specimen for a specimen measuring 120*12 mm.

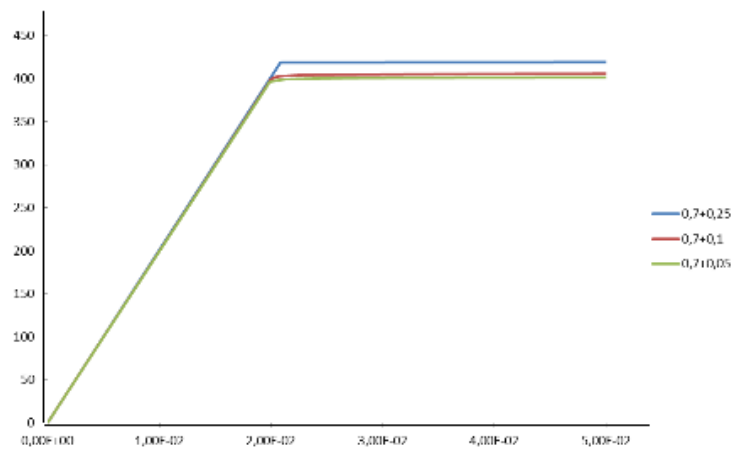The effect of coating thickness on the critical force of the sample is shown in the figure 3.

Fig. 2. Influence of coating thickness for samples 120*12.

The difference between the results obtained numerically and the experiments was substantiated, namely, the slope of the load-displacement curve. The figure below shows the experimental results and numerical results using flat and three-dimensional elements.

To check the numerical calculations, an analytical dependence was obtained:

$$U = \frac{P}{S_{\Sigma}E}L,$$

where U- displacement, P-load, L length of the working part, E - elastic modulus, S_{Σ} sample area. Shown in green on the graph.

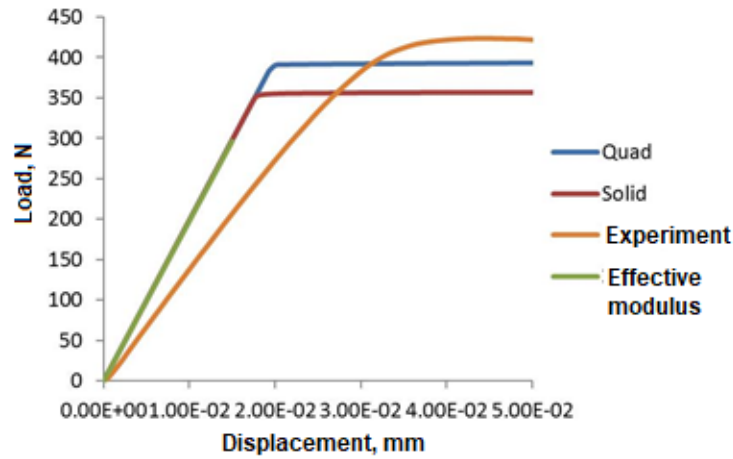The results for coated samples are given in Figure 3 and 4.
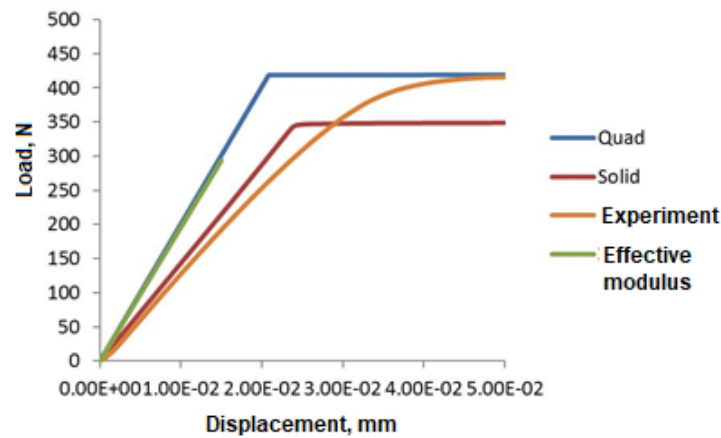
Fig. 3. Experiment results.

Fig. 4. Results of a numerical experiment.

As can be seen from Fig. 4, the value of the inclination angle obtained analytically coincides with the results obtained numerically using flat elements. The results obtained using three-dimensional elements differ significantly. It could be due to accumulating error.

This result shows that a model using flat elements gives a more accurate result than a model using three-dimensional elements.

The best agreement with experiment was shown by the results obtained in Ansys using Eigenvalue bucling, less than 1%. The worst agreement with the experiment was shown by the results obtained in Ansys using Solid-elements, about 70%.

4. Conclusion

The numerical results obtained for different elastic moduli showed that the deviation of the numerical curve from the experimental one is associated not with the physical and mechanical properties and geometric characteristics of the sample, but with the results obtained. Because the change in the displacement of the end of the sample was measured along the traverse, then the slope of the curve in this situation may not be true, and may not coincide with the slope obtained numerically. Also here one should take into account the fact that the loading rate of the sample was 2 times less than the loading rate to determine the elastic modulus.

References

1. Bodryshev, V.V., Babaytsev, A.V., Rabinskiy, L.N. Investigation of processes of deformation of plastic materials with the help of digital image processing// Periodico Tche Quimica, 2019, 16(33), p. 865–876.
2. Astapov, A.N., Kuznetsova, E.L., Rabinskiy, L.N. Operating capacity of anti-oxidizing coating in hypersonic flows of air plasma // Surface Review and Letters, 2019, 26(2), 1850145 p.
3. Babaytsev, A.V., Rabinskiy, L.N., Aung, K.T. Investigation of the contact zone of a cylindrical shell located between two parallel rigid plates with a gap //INCAS Bulletin, 2020, 12(Special Issue), p. 43–52.
4. Makarenko, A.V., Kuznetsova, E.L. Energy-Efficient Actuator for the Control System of Promising Vehicles //Russian Engineering Research. 2019. 39(9), p. 776-779.
5. Sha, M., Utkin, Y. A., Tushavina, O. V., Pronina, P. F. Experimental studies of heat and mass transfer from tip models made of carbon-carbon composite material (cccm) under conditions of high-intensity thermal load //Periodico Tche Quimica. 2020. vol.17, I. 35, pp 988-997.
6. Pronina, P.F., Tushavina, O.V., Starovoitov, E.I. Study of the radiation situation in moscow by investigating elastoplastic bodies in a neutron flux taking into account thermal effects // Periodico Tche Quimica, 2020, 17(35), p. 753–764.
7. Orekhov, A.A., Utkin, Y.A., Pronina, P.F. Determination of deformation in mesh composite structure under the action of compressive loads // Periodico Tche Quimica, 2020, 17(35), p. 599–608.
8. Dmitriev, V.G., Egorova, O.V., Starovoitov, E.I. Particularities of mathematical modeling of deformation processes for arched and panel designs of composites with large displacements and rotation angles //INCAS Bulletin, 2020, 12(Special Issue), p. 53–66.
9. Egorova, O.V., Starovoitov, E.I. Non-stationary diffraction problem of a plane oblique pressure wave on the shell in the form of a hyperbolic cylinder taking into account the dissipation effect // INCAS Bulletin, 2020, 12(Special Issue), p. 67–77.
10. Tushavina, O.V. Coupled heat transfer between a viscous shock gasdynamic layer and a transversely streamlined anisotropic half-space// INCAS Bulletin, 2020, 12 (Special Issue), p. 211–220.
11. Vakhneev, S., Starovoitov, E. Damping of circular composite viscoelastic plate vibration under neutron irradiation// Journal of Applied Engineering Science, 2020, 18(4), p. 699–704.
12. V.A. Pogodin, L.N. Rabinskii, S.A. Sitnikov. 3D Printing of Components for the Gas-Discharge Chamber of Electric Rocket Engines // Russian Engineering Research. 2019. Vol. 39, No. 9. p. 797-799.
13. Kyaw Y.K., Kuznetsova E.L., Makarenko A.V. Complex mathematical modelling of mechatronic modules of promising mobile objects// INCAS Bulletin, 2020, 12(Special Issue), p. 91-98.
14. Kuznetsova, L. E., Fedotenkov, V. G. Dynamics of a spherical enclosure in a liquid during ultrasonic cavitation // Journal of Applied Engineering Science. 2020. 18(4), p. 681 - 686.
15. Kuznetsova, E.L., Makarenko, A.V. Mathematic simulation of energy-efficient power supply sources for mechatronic modules of promising mobile objects// Periodico Tche Quimica, 2018, 15(Special Issue 1), p. 330-338.
16. Li, Y., Arutiunian, A.M., Kuznetsova, E.L., Fedotenkov, G.V. Method for solving plane unsteady contact problems for rigid stamp and elastic half-space with a cavity of arbitrary geometry and location // INCAS Bulletin, 2020, 12(Special Issue), p. 99–113.
17. Kuznetsova, E.L., Fedotenkov, G.V., Starovoitov, E.I. Methods of diagnostic of pipe mechanical damage using functional analysis, neural networks and method of finite elements // INCAS Bulletin, 2020, 12(Special Issue), p. 79–90.
18. Kyaw, Y.K., Pronina, P.F., Polyakov, P.O. Mathematical modelling of the effect of heat fluxes from external sources on the surface of spacecraft //Journal of Applied Engineering Science, 2020, 18(4), p. 732–736.
19. Bulychev N. A., Kuznetsova E.L., Bodryshev V. V. Rabinskiy L.N. Nanotechnological aspects of temperature-dependent decomposition of polymer solutions, Nanoscience and Technology: An International Journal, 2018, Vol. 9 (2), p. 91-97.
20. Bulychev, N.A., Rabinskiy, L.N., Tushavina, O.V. Effect of intense mechanical vibration of ultrasonic frequency on thermal unstable low-temperature plasma// Nanoscience and Technology: An International Journal, 2020, 11 (1), p. 15–21.

21. B.A. Garibyan. Mechanical Properties of Electroconductive Ceramics, International Journal of Pharmaceutical Research, 2020, Vol. 12, Supplementary Issue 2, pp. 1825-1828.
22. B.A. Garibyan. Enhancement of Mechanical Properties of Inorganic Glass under Ultrasonic Treatment, International Journal of Pharmaceutical Research, 2020, Vol. 12, Supplementary Issue 2, pp. 1829-1832.
23. B.A. Garibyan. Modelling of Technical Parameters of Discharge Reactor for Polymer Treatment, International Journal of Pharmaceutical Research, 2020, Vol. 12, Supplementary Issue 2, pp. 1833-1837.
24. N.A. Bulychev, A.V. Ivanov. Study of Nanostructure of Polymer Adsorption Layers on the Particles Surface of Titanium Dioxide, International Journal of Nanotechnology, 2019, Vol. 16, Nos. 6/7/8/9/10, pp. 356 – 365.
25. A.N. Tarasova. Vibration-based Method for Mechanochemical Coating Metallic Surfaces, International Journal of Pharmaceutical Research, 2020, Vol. 12, Supplementary Issue 2, pp. 1160-1168.
26. M.O. Kaptakov. Effect of Ultrasonic Treatment on Stability of TiO2 Aqueous Dispersions in Presence of Water-Soluble Polymers, International Journal of Pharmaceutical Research, 2020, Vol. 12, Supplementary Issue 2, pp. 1821-1824.
27. O.A. Butusova. Surface Modification of Titanium Dioxide Microparticles Under Ultrasonic Treatment, International Journal of Pharmaceutical Research, 2020, Vol. 12, I. 4, pp. 2292-2296.
28. A.N. Tarasova. Effect of Vibration on Physical Properties of Polymeric Latexes, International Journal of Pharmaceutical Research, 2020, Vol. 12, Supplementary Issue 2, pp. 1173-1180.
29. O.A. Butusova. Adsorption Behaviour of Ethylhydroxyethyl Cellulose on the Surface of Microparticles of Titanium and Ferrous Oxides, International Journal of Pharmaceutical Research, 2020, Vol. 12, Supplementary Issue 2, pp. 1156-1159.
30. Yu.V. Ioni. Synthesis of Metal Oxide Nanoparticles and Formation of Nanostructured Layers on Surfaces under Ultrasonic Vibrations, International Journal of Pharmaceutical Research, 2020, Vol. 12, Issue 4, pp. 3432-3435.
31. A.N. Tarasova. Effect of Reagent Concentrations on Equilibria in Water-Soluble Complexes, International Journal of Pharmaceutical Research, 2020, Vol. 12, Supplementary Issue 2, pp. 1169-1172.
32. Yu.V. Ioni, A. Ethiraj. Study of Microparticles Surface Modification by Electrokinetic Potential Measuring, International Journal of Pharmaceutical Research, 2020, Vol. 12, Issue 4, pp. 3436-3439.
33. N.A. Bulychev, M.A. Kazaryan. Optical Properties of Zinc Oxide Nanoparticles Synthesized in Plasma Discharge in Liquid under Ultrasonic Cavitation, Proceedings of SPIE, 2019, Vol. 11322, article number 1132219.
34. O.A. Butusova. Stabilization of Carbon Microparticles by High-Molecular Surfactants, International Journal of Pharmaceutical Research, 2020, Vol. 12, Supplementary Issue 2, pp. 1147-1151.
35. N.A. Bulychev, A.V. Ivanov. Effect of vibration on structure and properties of polymeric membranes, International Journal of Nanotechnology, 2019, Vol. 16, Nos. 6/7/8/9/10, pp. 334 – 343.
36. Yu.V. Ioni. Effect of Ultrasonic Treatment on Properties of Aqueous Dispersions of Inorganic and Organic Particles in Presence of Water-Soluble Polymers, International Journal of Pharmaceutical Research, 2020, Vol. 12, Issue 4, pp. 3440-3442.
37. O.A. Butusova. Vinyl Ether Copolymers as Stabilizers of Carbon Black Suspensions, International Journal of Pharmaceutical Research, 2020, Vol. 12, Supplementary Issue 2, pp. 1152-1155.
38. Yu.V. Ioni, A. Ethiraj. New Tailor-Made Polymer Stabilizers for Aqueous Dispersions of Hydrophobic Carbon Nanoparticles, International Journal of Pharmaceutical Research, 2020, Vol. 12, Issue 4, pp. 3443-3446.
39. Bulychev, N.A., Rabinskiy, L.N. Ceramic nanostructures obtained by acoustoplasma technique // Nanoscience and Technology: An International Journal, 2019, 10 (3), p. 279–286.
40. Yu.V. Ioni. Nanoparticles of noble metals on the surface of graphene flakes, Periodico Tche Quimica, 2020, Vol. 17, No. 36, pp. 1199-1211.
41. N.A. Bulychev, A.V. Ivanov. Nanostructure of Organic-Inorganic Composite Materials Based on Polymer Hydrogels, International Journal of Nanotechnology, 2019, Vol. 16, Nos. 6/7/8/9/10, pp. 344 – 355.

42. Formalev, V.F., Kartashov, É.M., Kolesnik, S.A. On the Dynamics of Motion and Reflection of Temperature Solitons in Wave Heat Transfer in Limited Regions // Journal of Engineering Physics and Thermophysics, 2020, 93(1), p. 10–15.

43. Formalev, V.F., Bulychev, N.A., Kuznetsova, E.L., Kolesnik, S.A. The Thermal State of a Packet of Cooled Microrocket Gas-Dynamic Lasers // Technical Physics Letters, 2020, 46(3), p. 245–248.

44. Rabinskiy, L.N., Tushavina, O.V., Formalev, V.F. Mathematical modeling of heat and mass transfer in shock layer on dimmed bodies at aerodynamic heating of aircraft// Asia Life Sciences, 2019, (2), p. 897–911.

45. Antufev, B.A., Egorova, O.V., Rabinskiy, L.N. Quasi-static stability of a ribbed shell interacting with moving load// INCAS Bulletin, 2019, 11, p. 33–39.

46. Rabinskiy, L.N., Tushavina, O.V., Starovoitov, E.I. Study of thermal effects of electromagnetic radiation on the environment from space rocket activity // INCAS Bulletin, 2020, 12 (Special Issue), p. 141–148.

47. Babaytsev, A.V., Orekhov, A.A., Rabinskiy, L.N. Properties and microstructure of AlSi10Mg samples obtained by selective laser melting// Nanoscience and Technology: An International Journal, 2020, 11(3), p. 213–222.

48. Egorova, O.V., Kyaw, Y.K. Solution of inverse non-stationary boundary value problems of diffraction of plane pressure wave on convex surfaces based on analytical solution//Journal of Applied Engineering Science, 2020, 18(4), p. 676–680.